



*J. Serb. Chem. Soc.* 86 (10) 971–982 (2021)  
JSCS–5476

## Sodium ion chemosensor of 3-oxo-3*H*-benzo[*f*]chromene-2-carboxylic acid: An experimental and computational study

JAMALUDIN AL-ANSHORI\*, ANDI RAHIM, AJAR FAFLUL ABROR,  
IKA WIANI HIDAYAT, TRI MAYANTI, MUHAMMAD YUSUF,  
JULIANDRI JULIANDRI and ACE TATANG HIDAYAT

*Department of Chemistry, Faculty of Mathematics and Natural Sciences, Universitas Padjadjaran, Jl. Raya Jatinangor km.21 Bandung-Sumedang, Jatinangor, 40133, Indonesia*

(Received 29 September 2020, revised 5 March, accepted 23 March 2021)

**Abstract:** A fluorescence compound with the typical skeleton of benzocoumarin was synthesized and its interaction with various metal ions was evaluated. The synthesis was performed *via* Knoevenagel condensation whereas identification of the product was accomplished by various spectroscopic techniques. The chemosensor test against representative metal ions was monitored by fluorescence spectrophotometry. A density functional theory calculation (DFT, functional/basis set; M06/6-31G (d, p)) was also performed to clarify the experimental results and to confirm the mechanism of interaction. 3-Oxo-3*H*-benzo[*f*]chromene-2-carboxylic acid **1** was obtained as a yellow solid in 60 % chemical yield. Melting point; 235.6–236.7 °C and  $\lambda_{\max}$  UV/Vis,  $\lambda_{\text{em}}$  and Stokes shift (MeOH, nm) of 374, 445 and 71 nm, respectively. The structure of the compound was identified based on spectroscopic data and literature comparison. Compound **1** exhibited a chelation quenched fluorescence (CHQF) phenomenon selectively toward the Na<sup>+</sup>, with a binding stoichiometry (1:2) and *LoD* and *LoQ* of 0.14 and 0.48 mg/L, respectively. Based on DFT calculations, compound **1** chelated Na<sup>+</sup> through mechanism of oxidative (1:1 equivalent) and reductive (2:1 equivalent) photoinduced electron transfer (PET), correspondingly.

**Keywords:** benzocoumarin; fluorescence; CHQF; DFT; PET.

### INTRODUCTION

Discovering new ion sensors and molecular recognition has gained increased consideration due to their prospective applications in analytical chemistry, life science, catalysis and environmental monitoring.<sup>1–6</sup> In particular, the ion fluorescence sensing based technique shows more prominent features than other methods, such as AAS,<sup>7</sup> ICP spectroscopy,<sup>8,9</sup> analysis based on neutron

\* Corresponding author. E-mail: jamaludin.al.anshori@unpad.ac.id  
<https://doi.org/10.2298/JSC200929022A>



activation,<sup>10</sup> chromatography,<sup>11</sup> voltammetry<sup>12</sup> and others<sup>13–15</sup> as it conserves inherent sensitivity and selectivity, low cost, handiness, spatial and temporal monitoring with instant response times.<sup>16</sup> Among various metal ions, sodium is predominantly attractive to current researchers, as it is one of the most abundant metals in the environment and in biology, playing critical ecological and physiological roles. To the best of our knowledge, Na<sup>+</sup> chemosensors based on such fluorescence platforms as BODIPY,<sup>17</sup> rhodol,<sup>18</sup> anthracene and azo,<sup>19</sup> ether and aza crown derivatives,<sup>20</sup> indole,<sup>21</sup> benzophosphole,<sup>22</sup> and calix[4]arene<sup>23</sup> have all been explored. A relatively unexplored class of fluorescent platform for sodium ion sensing is benzocoumarin which has better photophysical properties than basic coumarin.<sup>24</sup> Furthermore, the synthetic pathway is simple and straightforward through Pechmann,<sup>25</sup> and Knoevenagel<sup>26</sup> condensation. Accordingly, a known fluorescent benzocoumarin-type compound was synthesized and its chemosensory properties against sodium ion reported for the first time. In addition, a computational study of the chemosensor was performed herein.

## EXPERIMENTAL

### *Materials and methods*

P. a. grade chemicals, purchased from Sigma–Aldrich and Merck, were used. All glassware apparatus was oven-dried prior to use. <sup>1</sup>H- and <sup>13</sup>C-NMR spectra were obtained on Agilent 500 and 126 MHz spectrometers, respectively, in DMSO-*d*<sub>6</sub>. The NMR signals were referenced to the residual peak of the (major) solvent. The deuterated solvents were stored over activated 3 Å molecular sieves (8–12 mesh) under dry N<sub>2</sub>. UV/Vis absorption spectra and their molar absorptivity were measured on a Shimadzu 8400 UV/Vis spectrometer with matched 1.0 cm quartz cells. The spectra were recorded over 0.1 nm interval data. Emission spectra were recorded on an automated Fluorescence Agilent G9800A Cary Eclipse spectrometer in 1.0 cm quartz fluorescence cuvettes at 25 °C. The slit of the excitation and emission slits were set to 5 nm, while the scanning rate was 600 nm min<sup>-1</sup> with interval data of 1 nm. The sample concentration was adjusted to preserve the absorbance below 0.1 at λ<sub>max</sub>; each sample was measured three times and the spectra were averaged. Infrared spectra were obtained on a Perkin Elmer FTIR instrument in potassium bromide (KBr) pellets. Relative masses were recorded on a mass spectrometer (Waters high resolution-time of flight-MS Lockspray/HR-TOF-MS) in the positive and negative ion mode. The melting points were determined on an uncorrected MP55 electrothermal melting point apparatus in open-end capillary tubes. DFT calculations were performed on a PC with Processor Intel® Xeon (R) CPU E5-2650 v2@2.60 GHz ×32, RAM 16 GB. The calculations were performed using the Gaussian 09 program<sup>27</sup> at the M06 hybrid meta exchange correlation density functional at the 6-31G(d, p) level of theory.<sup>28</sup> Furthermore, the structure of chemosensor was optimized with and without M<sup>+</sup> to confirm their stability, by comparing their frequency values. Frontier molecular orbital analysis was accomplished to confirm the results of the experiment<sup>43</sup> as well as the interaction mechanism of chemosensor with the metal ion.

### *Synthesis of 3-oxo-3H-benzo[f]chromene-2-carboxylic acid (1)*

The synthesis of compound **1** was carried out as in Scheme 1. The synthesis method was based on procedure reported by Xiao *et al.*<sup>29</sup> 2-Hydroxy-naphthaldehyde **2** (100 mg, 0.58

mmol) and meldrum's acid **3** (60.5 mg, 0.58 mmol) were dissolved in a two-neck, round-bottom flask with 15 mL of ethanol. A drop of pyridine was added to the mixture and then refluxed for 2–4 h at 80 °C. Afterwards, the reaction mixture was kept at ambient temperature for 24 h. The precipitated solid was filtered and washed several times with ethanol to yield a pure yellowish solid (83 mg, 60 %).

The analytical and spectral data of the compound are given in the Supplementary material to this paper.

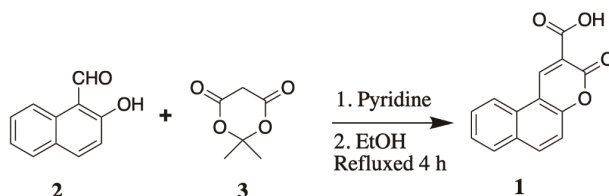
#### Method of metal ion sensing of 3-oxo-3H-benzo[f]chromene-2-carboxylic acid (**1**)

The method was adopted from procedure reported by Piao *et al.*<sup>30</sup> and Amirnasr *et al.*<sup>31</sup> A stock solution of compound **1** ( $4.17 \times 10^{-3}$  mol dm<sup>-3</sup>) was prepared in methanol, while stock solution of representative metal ions ( $1-10 \times 10^{-3}$  mol dm<sup>-3</sup>) was dissolved in milli-Q water. Some metal ions such as, Na<sup>+</sup>, Li<sup>+</sup>, Mg<sup>2+</sup>, Ni<sup>2+</sup>, and Cu<sup>2+</sup> were used as sulfate whereas some others like, K<sup>+</sup>, Cd<sup>2+</sup>, Ag<sup>+</sup>, Al<sup>3+</sup>, Pb<sup>2+</sup>, and Cr<sup>3+</sup> were used as nitrate. The stock solution of **1** was mixed with solution of various metal ions in 5 mL volumetric flask at mole ratio of 1:9 to 9:1 (**1**:metal ion) by keeping constant total concentration. Binding stoichiometry was calculated based on Job's plot experiment,<sup>32</sup> while selectivity experiment was accomplished by mixing 1 molar of compound **1** with 6 molar equivalents of Na<sup>+</sup> in the presence of each 6 molar equivalents of an interference ion. All fluorescence spectra were recorded at excitation wavelength of 361 nm and the temperature was 20 °C.

## RESULTS AND DISCUSSION

#### Synthesis of 3-oxo-3H-benzo[f]chromene-2-carboxylic acid (**1**)

Knoevenagel condensation of **2** and **3** over basic catalyst of pyridine resulted in a 60 % chemical yield of 3-oxo-3H-benzo[f]chromene-2-carboxylic acid **1** (Scheme 1).



Scheme 1. Synthesis of **1**, 3-oxo-3H-benzo[f]chromene-2-carboxylic acid.

Instead of Pechmann condensation,<sup>25</sup> this pathway was one of the common method to form coumarin skeleton through intramolecular heterocyclization between an active hydrogen compound of meldrum's acid with an  $\alpha$ -hydroxy aldehyde in the presence of a basic catalyst.<sup>26</sup> In general, the achieved product has similar properties to those obtained by Xiao *et al.*<sup>29</sup>

The infrared spectrum of **1** (Fig. S-1 of the Supplementary material) showed typical carboxylic acid absorbances at 3420 (broad weak) and 1750 cm<sup>-1</sup> (sharp medium), which belong to stretching vibrations of the –OH and C=O moieties, respectively. The appearance of ester lactone was characterized by the vibration of C=O and C–O at 1683 and 1218 cm<sup>-1</sup> (sharp strong), correspondingly. The naphthalene moiety was confirmed by the stretching vibration of C–H sp<sup>2</sup> (sharp

medium) at  $3058\text{ cm}^{-1}$  and C=C aryl (sharp strong) at  $1571\text{ cm}^{-1}$ . To clarify the data,  $^1\text{H-NMR}$  and  $^{13}\text{C-NMR}$  were recorded in aprotic solvent of  $\text{DMSO-}d_6$  (Figs. S-2 and S-3 of the Supplementary material). Seven different types of protons were observed in the spectrum. One proton resonance at 9.34 ppm was attributed to the alkene proton of H-14 and the other six resonances at 7.59–8.57 ppm were recognized as aromatic naphthalene protons. In addition, 13 different types of carbons appeared in the  $^{13}\text{C-NMR}$  spectrum. The signals were attributed to one olefinic carbon at 112.50 ppm, nine aryl carbons at 116.94, 117.94, 122.77, 126.88, 129.45, 129.50, 130.27, 136.30 and 144.18 ppm, one oxygenated aryl carbon at 155.49 ppm, one lactone carbonyl at 157.24 ppm, and one carboxylic acid carbonyl at 164.78 ppm. All NMR data were in agreement with those reported by Fu *et al.* (Tables S-I and S-II of the Supplementary material).<sup>33</sup> Finally, the molecular formula of **1** was confirmed as  $\text{C}_{14}\text{H}_8\text{O}_4$  by HR-TOF-MS ( $\text{ES}^-$  and  $\text{ES}^+$ , Fig. S-4 of the Supplementary material).

*Photophysical properties of 3-oxo-3H-benzo[f]chromene-2-carboxylic acid (1)*

Compound **1** showed strong absorption ( $\lambda_{\text{max}}$ ) and emission maximum ( $\lambda_{\text{em}}$ ) in methanol at 374 and 445 nm, respectively (Fig. 1). The typical maxima ranged within the benzocoumarin scaffold absorption and emission spectra at 355–488 and 400–625 nm, correspondingly.<sup>26</sup>

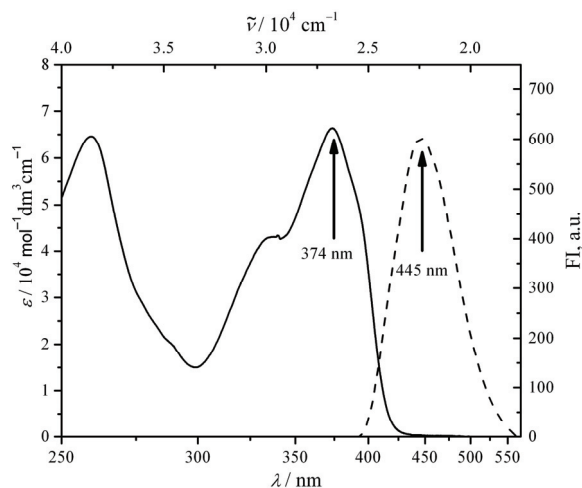


Fig. 1. Spectra of UV/Vis (solid line) and emission (dash line),  $\lambda_{\text{ex}} 361\text{ nm}$ , of **1** ( $8 \times 10^{-6}\text{ mol dm}^{-3}$ ) in MeOH.

Compared to the spectral properties of the basic coumarin skeleton, the extended conjugated  $\pi$  system of **1** was not only able to shift the maxima bathochromically by 20–50 nm but also increase its absorptivity by more than 10 times. In addition, intermolecular hydrogen bonding between methanol and carbonyl

moieties of such coumarine compound allowed an intramolecular charge transfer (ICT)<sup>34</sup> and red shifted the emission spectra of **1**.<sup>35</sup> Thus, the Stokes shift of compound **1** was relatively large as 71 nm. Overall, the benzocoumarin system improved optical properties of the coumarin system, which could overcome the limitations such as, photobleaching, photodamage, and shallow tissue penetration depth in bioimaging application.<sup>36–39</sup>

*Chemosensor properties of 3-oxo-3H-benzo[f]chromene-2-carboxylic acid (1) against various metal ions*

The interaction of **1** with representative metal ions ( $\text{Li}^+$ ,  $\text{Na}^+$ ,  $\text{K}^+$ ,  $\text{Mg}^{2+}$ ,  $\text{Ag}^+$ ,  $\text{Cu}^{2+}$ ,  $\text{Pb}^{2+}$ ,  $\text{Ni}^{2+}$ ,  $\text{Cd}^{2+}$ ,  $\text{Cr}^{3+}$  and  $\text{Al}^{3+}$ ) was monitored qualitatively through visual observation of the metal-induced fluorescence quenching under a 365 nm UV lamp and quantitatively by fluorescence spectrophotometry in a mixture of MeOH:H<sub>2</sub>O (2:8 volume ratio) at room temperature. Upon addition of respective equimolar quantities of metal ions, *i.e.*,  $\text{Li}^+$ ,  $\text{Na}^+$ ,  $\text{K}^+$ ,  $\text{Mg}^{2+}$ ,  $\text{Ag}^+$ ,  $\text{Cu}^{2+}$ ,  $\text{Pb}^{2+}$ ,  $\text{Ni}^{2+}$ ,  $\text{Cd}^{2+}$ ,  $\text{Cr}^{3+}$  and  $\text{Al}^{3+}$ , to a  $2.28 \times 10^{-6}$  mol dm<sup>-3</sup> solution of **1**, it was found that only  $\text{Na}^+$  induced blue fluorescence quenching of **1** (Figs. 2 and 3) with a binding stoichiometry of 1:2 (Fig. S-5 of the Supplementary material).

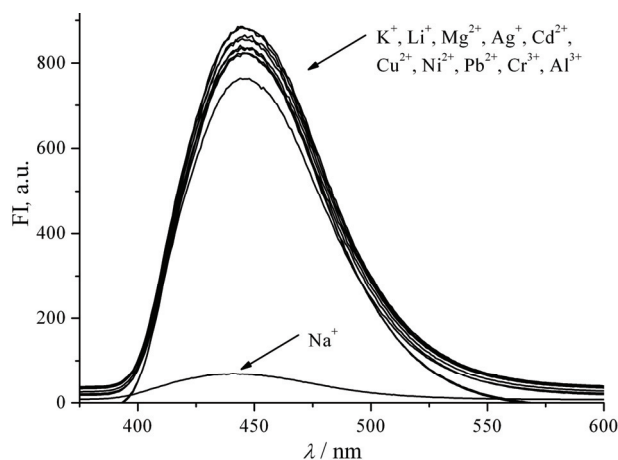


Fig. 2. Fluorescence spectra of **1** ( $2.28 \times 10^{-6}$  mol dm<sup>-3</sup>) before and after addition of 6 molar equivalents of various metal ions ( $\lambda_{\text{ex}} = 361$  nm,  $\lambda_{\text{em}} = 455$  nm).

Upon titration of **1** with sodium ions, red shifts of the emission spectra of the **1** +  $\text{Na}^+$  complex were revealed up to  $\pm 10$  nm compared to the original emission maxima of **1** (445 nm, Fig. 3). This implies that a dipolar interaction was formed between the complex of **1**+ $\text{Na}^+$  and the polar solvent of MeOH:H<sub>2</sub>O (2:8) and thus, the energy of the excited state decreased and the maxima shifted to a longer wavelength.<sup>40</sup> Furthermore, based on the linear equation, obtained from the calibration curve of **1** against various concentration of sodium ion (Fig. S-6 of the

Supplementary material), the *LoD* and *LoQ* of **1** were found to be 0.14 and 0.48 mg L<sup>-1</sup>, respectively.

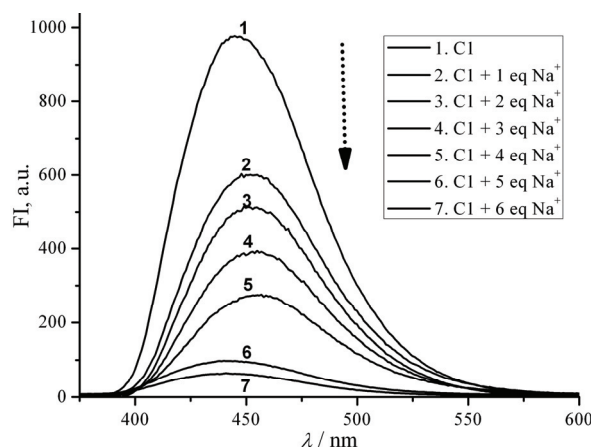


Fig. 3. The changes of fluorescence spectra of **1** (C1;  $2.28 \times 10^{-6}$  mol dm<sup>-3</sup>) after addition of 1–6 molar equivalents of Na<sup>+</sup> in MeOH:H<sub>2</sub>O (2:8, volume ratio);  $\lambda_{\text{ex}} = 361$  nm,  $\lambda_{\text{em}} = 455$  nm.

In fact, based on qualitative observation under UV light at 365 nm, the fluorescence intensity of **1** was actually totally quenched by other metal ions but at equimolar quantities of 15 to more than 500 (Fig. S-7 of the Supplementary material). In general, the fluorescence quenching was attributed to the metal ion chelation with the donor atom of carboxylate O in **1**, known as a chelation-quenched fluorescence (CHQF) effect. The phenomenon is due to electron transfer from the LUMO of the excited fluorophore to the vacant s-orbital of metal ion,<sup>41</sup> which promotes intermolecular charge transfer (ICT). The competitive experiment to further estimate selectivity of **1** against Na<sup>+</sup> in the presence of other metal ions including Li<sup>+</sup>, K<sup>+</sup>, Mg<sup>2+</sup>, Ag<sup>+</sup>, Cu<sup>2+</sup>, Pb<sup>2+</sup>, Ni<sup>2+</sup>, Cd<sup>2+</sup>, Cr<sup>3+</sup>, and Al<sup>3+</sup> was accomplished under the same conditions (Fig. 4). It was clearly noticeable that the presence of Na<sup>+</sup> among other metal ions showed immediate response in quenching of fluorescence. The result revealed that recognition of Na<sup>+</sup> by **1** was relatively not influenced by other competitive metal ions.

*Computational study of chemosensory mechanism of 3-oxo-3H-benzo[f]chromene-2-carboxylic acid (1) against sodium metal ion*

To understand selectivity of compound **1** against sodium ion and its mechanism, DFT calculations were performed and analyzed using the Gaussian 09W program. Since an intermolecular charge transfer (ICT) between a chemosensor and a metal ion plays essential role during chelating processes,<sup>42</sup> the calculation was pointed to the energy gap of HOMO–LUMO of compound **1** against the sodium ion.

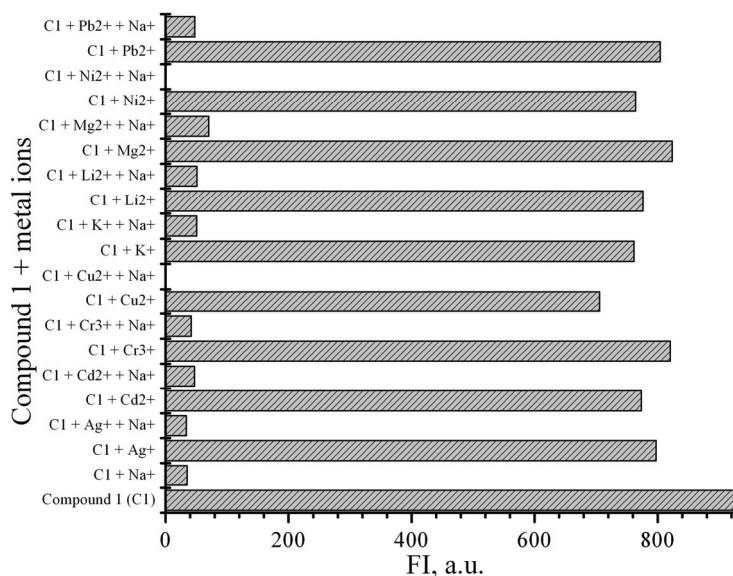


Fig. 4. Fluorescence intensity of compound **1** (C1;  $2.28 \times 10^{-6}$  mol dm $^{-3}$ ) with various metal ions (Ag $^{+}$ , Cd $^{2+}$ , Cr $^{3+}$ , Cu $^{2+}$ , Pb $^{2+}$ , K $^{+}$ , Li $^{2+}$ , Mg $^{2+}$ , Ni $^{2+}$ ) in MeOH:H $_2$ O (2:8 volume ratio) in the presence of Na $^{+}$  (1:6 molar equivalents;  $\lambda_{\text{ex}} = 361$  nm,  $\lambda_{\text{em}} = 455$  nm).

In geometry optimization of **1**, the minimum state was used to obtain a stable structure of the compound, which could be observed from its positive frequency value (Table S-III of the Supplementary material). Furthermore, frontier molecular orbital (FMO) analysis of optimized **1** (Fig. S-8 of the Supplementary material) confirmed that compound **1**, which has a lower  $E_{\text{HOMO}}$  of receptor than the  $E_{\text{HOMO}}$  of the fluorophore, emitted the fluorescence. On the other hand, upon chelation toward the Na $^{+}$  (Fig. 5), compound **1** exhibited fluorescence quenching process, as described in Figs. 6 and 7.

FMO analysis of the optimized **1** against Na $^{+}$  (purple) with ratios 1:1 and 2:1, clearly distinguished typical photoinduced electron transfer occurred in the chelating compound **1** + Na $^{+}$ .

According to Fig. 6, when ratio of compound **1** to Na $^{+}$  was 1:1, fluorescence quenching was allowed upon transfer of an excited electron of fluorophore to the LUMO of receptor and finally to the HOMO of the fluorophore. The electron transfer, identified as oxidative PET, $^{43}$  was plausibly occurring if the energy gap of the LUMO of the fluorophore and receptor (0.631 eV) was lower than the energy gap of the HOMO–LUMO of the fluorophore (4.347 eV).

On the other hand, when the ratio of compound **1** to Na $^{+}$  was 2:1 (Fig. 7), quenching occurred through transfer of a HOMO electron of the receptor to the HOMO of the excited fluorophore. The process, identified as reductive PET, $^{42}$  was probably occurring if the energy gap of the HOMO of the fluorophore and

receptor (0.336 eV) was lower than the HOMO–LUMO energy gap of the fluorophore (4.362 eV).

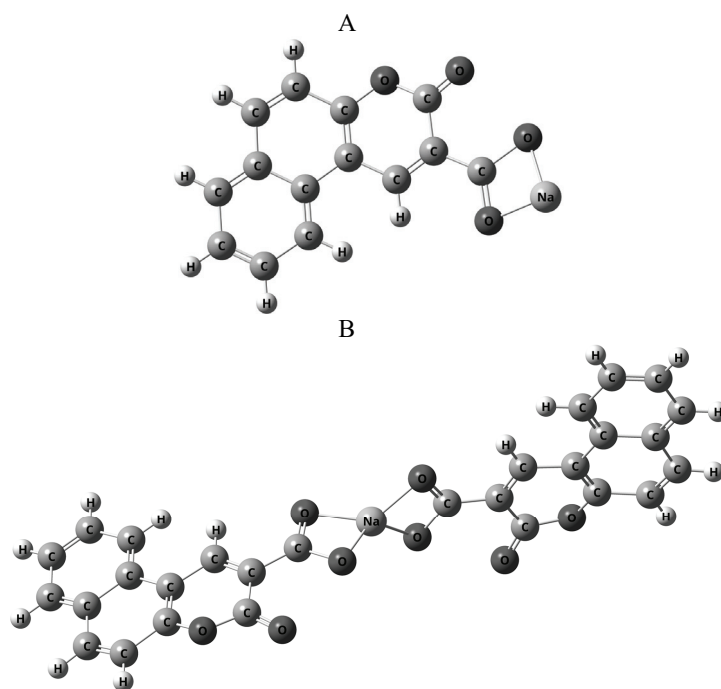


Fig. 5. Structure modeling of **1** against  $\text{Na}^+$ ; A) 1:1; B) 2:1.

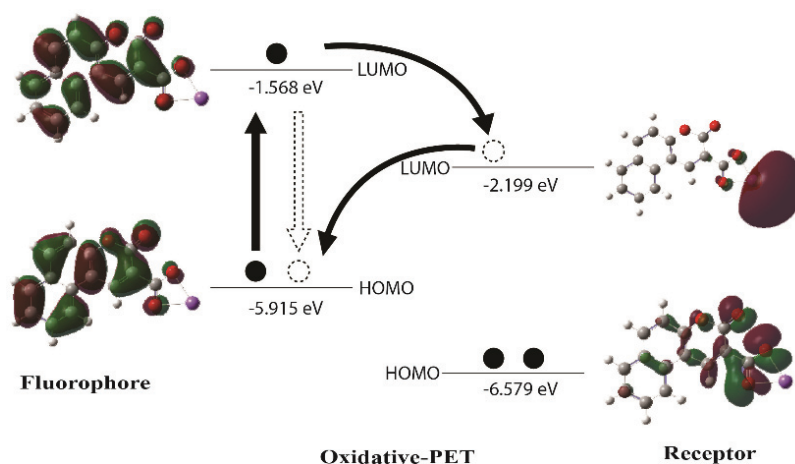


Fig. 6. Calculated frontier molecular orbitals of compound **1** +  $\text{Na}^+$  (1:1) and the corresponding interaction of HOMO and LUMO orbital *via* oxidative-PET.



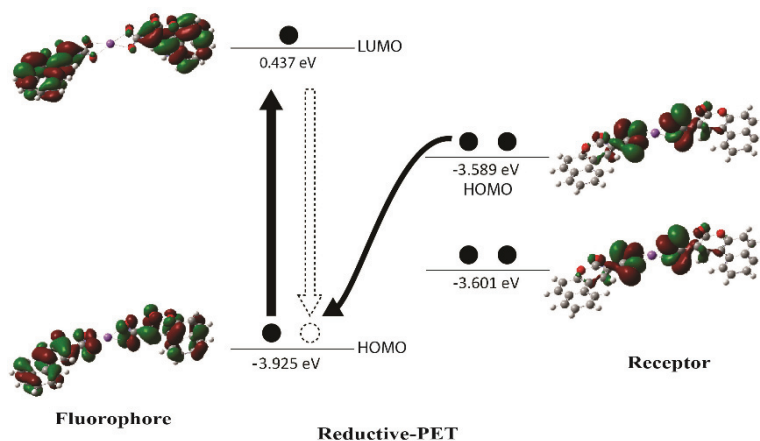


Fig. 7. Calculated frontier molecular orbitals of compound **1** + Na<sup>+</sup> (2:1) and the corresponding interaction of the HOMO and LUMO orbitals *via* reductive-PET.

Overall, the theoretical calculation was in accordance with the experimental results. Furthermore, the interaction mechanism was clearly resolved *in silico*.

#### CONCLUSIONS

The benzocoumarin typical compound, 3-oxo-3*H*-benzo[*f*]chromene-2-carboxylic acid (**1**) was successfully synthesized in 60 % chemical yield. The compound showed prominent sensory properties against Na<sup>+</sup> selectively through oxidative and reductive PET mechanisms. The *LoD* and *LoQ* **1** against Na<sup>+</sup> in MeOH:H<sub>2</sub>O (2:8 volume ratio) were 0.14 and 0.48 mg/L, respectively. Thus, the compound was suggested as potential chemosensor of Na<sup>+</sup> ion in aqueous systems.

#### SUPPLEMENTARY MATERIAL

Additional data and information are available electronically at the pages of journal website: <https://www.shd-pub.org.rs/index.php/JSCS/article/view/9945>, or from the corresponding author on request.

*Acknowledgements.* This work was supported by KEMENRISTEK DIKTI research grant (No.1827/UN6.3.1/LT/2020) and ALG grant of Prof. Ace T. Hidayat (No.1427/UN6.3.1/LT/2020).

#### ИЗВОД

#### НАТРИЈУМСКИ ХЕМОСЕНЗОР 3-ОКСО-3*H*-БЕНЗО[*f*]ХРОМЕН-2-КАРБОКСИЛНА КИСЕЛИНА: ЕСПЕРИМЕНТАЛНА И КОМПЈУТЕРСКА СУДИЈА

JAMALUDIN AL-ANSHORI, ANDI RAHIM, AJAR FAFLUL ABROR, IKA WIANI HIDAYAT, TRI MAYANTI, MUHAMMAD YUSUF, JULIANDRI JULIANDRI и ACE TATANG HIDAYAT

Department of Chemistry, Faculty of Mathematics and Natural Sciences, Universitas Padjadjaran Jl. Raya Jatinangor km.21 Bandung-Sumedang, Jatinangor, 40133, Indonesia

Синтетисано је флуоресцентно једињење бензокумаринске структуре и иститивана је његова интеракција са различитим металима. Синтеза је изведена примером *Knoeven-*

*agel* кондензације, док је идентификација производа урађена примером различитих спектроскопних техника. Хемосензор је тестиран са репрезентативним јонима метала флуоресцентом спектроскопијом. Примењена је и теорија функционала густине (DFT), ради појашњавања експерименталних резултата и потврде механизме реакције. Добијена је 3-оксо-3*H*-бензо[*f*]хромен-2-карбоксилна киселина (**1**), као жута супстанца са приносом од 60 %, тачком топљења од 235,6–236,77 °C,  $\lambda_{\max}$  UV/Vis,  $\lambda_{\text{em}}$  и Stokes померањем (MeOH, nm) на 374, 445 и 71 nm, редом. Структура једињења је идентификована на основу поређења спектроскопских и података из литературе. Једињење **1** испољава феномен хелационог гашења флуоресценције (CHQF) селективно према Na<sup>+</sup>, са стехиометријом 1:2 и лимитима детекције и квантификације од 0,14 и 0,48 mg/L. На основу DFT калкулације, једињење **1** хелира Na<sup>+</sup> механизмима оксидативног (1:1) и редуктивног (2:1) фотоиндукованог електронског трансфера (PET).

(Примљено 29. септембра 2020, ревидирано 5. марта, прихваћено 23. марта 2021)

#### REFERENCES

1. C. Zhou, N. Xiao, Y. Li, *Can. J. Chem.* **92** (2014) 1092 (<https://dx.doi.org/10.1139/cjc-2014-0011>)
2. J. S. Kim, D. T. Quang, *Chem. Rev.* **107** (2007) 3780 (<https://dx.doi.org/10.1021/cr068046j>)
3. H. N. Kim, M. H. Lee, H. J. Kim, J. S. Kim, J. Yoon, *Chem. Soc. Rev.* **37** (2008) 1465 (<http://dx.doi.org/10.1039/B802497A>)
4. X. Chen, T. Pradhan, F. Wang, J. S. Kim, J. Yoon, *Chem. Rev.* **112** (2012) 1910 (<https://doi.org/10.1021/cr200201z>)
5. J. F. Clark, D. L. Clark, G. D. Whitener, N. C. Schroeder, S. H. Strauss, *Environ. Sci. Technol.* **30** (1996) 3124 (<https://dx.doi.org/10.1021/es960394n>)
6. M. P. Anderson, R. J. Gregory, S. Thompson, D. W. Souza, S. Paul, R. C. Mulligan, A. E. Smith, M. J. Welsh, *Science* **80** **253** (1991) 202 (<https://dx.doi.org/10.1126/science.1712984>)
7. Y. Yamini, N. Alizadeh, M. Shamsipur, *Anal. Chim. Acta* **355** (1997) 69 ([https://dx.doi.org/10.1016/S0003-2670\(97\)81613-3](https://dx.doi.org/10.1016/S0003-2670(97)81613-3))
8. C.F. Harrington, S.A. Merson, T. M. D. D'Silva, *Anal. Chim. Acta* **505** (2004) 247 (<https://dx.doi.org/10.1016/j.aca.2003.10.046>)
9. S. L. C. Ferreira, A. S. Queiroz, M. S. Fernandes, H. C. dos Santos, *Spectrochim. Acta, B* **57** (2002) 1939–1950 ([https://dx.doi.org/10.1016/S0584-8547\(02\)00160-X](https://dx.doi.org/10.1016/S0584-8547(02)00160-X))
10. J. C. Yu, J. M. Lo, C. M. Wai, *Anal. Chim. Acta* **154** (1983) 307 ([https://dx.doi.org/10.1016/0003-2670\(83\)80032-4](https://dx.doi.org/10.1016/0003-2670(83)80032-4))
11. A. Ali, H. Shen, X. Yin, *Anal. Chim. Acta* **369** (1998) 215 ([https://doi.org/10.1016/S0003-2670\(98\)00252-9](https://doi.org/10.1016/S0003-2670(98)00252-9))
12. A. Bobrowski, K. Nowak, J. Zarebski, *Anal. Bioanal. Chem.* **382** (2005) 1691 (<https://dx.doi.org/10.1007/s00216-005-3313-2>)
13. S. Karthikeyan, V. K. Gupta, R. Boopathy, A. Titus, G. Sekaran, *J. Mol. Liq.* **173** (2012) 153 (<https://dx.doi.org/10.1016/j.molliq.2012.06.022>)
14. V. K. Gupta, S. Kumar, R. Singh, L. P. Singh, S. K. Shoora, B. Sethi, *J. Mol. Liq.* **195** (2014) 65 (<https://dx.doi.org/10.1016/j.molliq.2014.02.001>)
15. G. Dimeski, T. Badrick, A. S. John, *Clin. Chim. Acta* **411** (2010) 309 (<https://dx.doi.org/10.1016/j.cca.2009.12.005>)
16. N. Mergu, A. K. Singh, V. K. Gupta, *Sensors* **15** (2015) 9097 (<https://doi.org/10.3390/s150409097>)

17. K. Yamada, Y. Nomura, D. Citterio, N. Iwasawa, K. Suzuki, *J. Am. Chem. Soc.* **127** (2005) 6956 (<https://dx.doi.org/10.1021/ja042414o>)
18. Y. M. Poronik, G. Clermont, M. Blanchard-Desce, D. T. Gryko, *J. Org. Chem.* **78** (2013) 11721 (<https://dx.doi.org/10.1021/jo401653t>)
19. T. Gunnlaugsson, M. Nieuwenhuyzen, L. Richard, V. Thoss, *J. Chem. Soc. Perkin Trans. 2* (2002) 141 (<http://dx.doi.org/10.1039/B106474F>)
20. P. Nandhikonda, M. P. Begaye, M. D. Heagy, *Tetrahedron Lett.* **50** (2009) 2459 (<https://dx.doi.org/10.1016/j.tetlet.2009.02.197>)
21. W. Zhou, J. Ding, J. Liu, *Nucleic Acids Res.* **44** (2016) 10377 (<https://dx.doi.org/10.1093/nar/gkw845>)
22. M. Taki, H. Ogasawara, H. Osaki, A. Fukazawa, Y. Sato, K. Ogasawara, T. Higashiyama, S. Yamaguchi, *Chem. Commun.* **51** (2015) 11880 (<https://dx.doi.org/10.1039/c5cc03547c>)
23. I. Leray, J.-P. Lefèvre, J.-F. Delouis, J. Delaire, B. Valeur, *Chem. Eur. J.* **7** (2001) 4590 ([https://doi.org/10.1002/1521-3765\(20011105\)7:21%3C4590::AID-CHEM4590%3E3.0.CO;2-A](https://doi.org/10.1002/1521-3765(20011105)7:21%3C4590::AID-CHEM4590%3E3.0.CO;2-A))
24. N. A. Al-Masoudi, N. J. Al-Salihi, Y. A. Marich, *J. Fluoresc.* **25** (2015) 1847 (<https://dx.doi.org/10.1007/s10895-015-1677-z>)
25. J. Al Anshori, D. S. Rahayu, A. T. Hidayat, I. W. Hidayat, A. Zainuddin, *Res. J. Chem. Environ.* **22** (2018) 91 (<https://worldresearchersassociations.com/SpecialIssueAugust2018.aspx>)
26. M. Tasior, D. Kim, S. Singha, M. Krzeszewski, K. H. Ahn, D. T. Gryko, *J. Mater. Chem. C* **3** (2015) 1421 (<https://dx.doi.org/10.1039/C4TC02665A>)
27. *Gaussian 16, Revision C.01*, Gaussian, Inc., Wallingford, CT, 2016 (<https://gaussian.com>)
28. Y. Zhao, D. G. Truhlar, *Theor. Chem. Accounts* **120** (2008) 215 (<https://dx.doi.org/10.1007/s00214-007-0310-x>)
29. J. M. Xiao, L. Feng, L. S. Zhou, H. Z. Gao, Y. L. Zhang, K. W. Yang, *Eur. J. Med. Chem.* **59** (2013) 150 (<https://dx.doi.org/10.1016/j.ejmech.2012.11.019>)
30. J. Piao, J. Lv, X. Zhou, T. Zhao, X. Wu, *Spectrochim. Acta, A* **128** (2014) 475 (<https://dx.doi.org/10.1016/j.saa.2014.03.002>)
31. M. Amiras, R. Sadeghi Erami, S. Meghdadi, *Sensors Actuators, B* **233** (2016) 355 (<https://dx.doi.org/10.1016/j.snb.2016.04.077>)
32. S. Goswami, S. Chakraborty, S. Paul, S. Halder, S. Panja, S. K. Mukhopadhyay, *Org. Biomol. Chem.* **12** (2014) 3037 (<https://dx.doi.org/10.1039/C4OB00067F>)
33. X. B. Fu, X. F. Wang, J. N. Chen, D. W. Wu, T. Li, X. C. Shen, J. K. Qin, *Molecules* **20** (2015) 18565 (<https://doi.org/10.3390/molecules201018565>)
34. W. Zhao, L. Pan, W. Bian, J. Wang, *Chem. Phys. Chem.* **9** (2008) 1593 (<https://dx.doi.org/10.1002/cphc.200800131>)
35. X. Liu, J. M. Cole, K. S. Low, *J. Phys. Chem., C* **117** (2013) 14731 (<https://dx.doi.org/10.1021/jp310397z>)
36. R. Wang, F. Zhang, *J. Mater. Chem., B* **2** (2014) 2422 (<https://dx.doi.org/10.1039/C3TB21447H>)
37. T. G. Phan, A. Bullen, *Immunol. Cell Biol.* **88** (2010) 438 (<https://doi.org/10.1038/icb.2009.116>)
38. B. P. Joshi, T. D. Wang, *Cancers* **2** (2010) 1251 (<https://dx.doi.org/10.3390/cancers2021251>)
39. J. Rao, A. Dragulescu-Andrasi, H. Yao, *Curr. Opin. Biotechnol.* **18** (2007) 17 (<https://dx.doi.org/10.1016/j.copbio.2007.01.003>)

40. R. Macgregor, G. Weber, *Ann. N.Y. Acad. Sci.* **366** (1981) 140  
(<https://doi.org/10.1111/j.1749-6632.1981.tb20751.x>)
41. A. T. Afaneh, G. Schreckenbach, *J. Phys. Chem., A* **119** (2015) 8106  
(<https://dx.doi.org/10.1021/acs.jpca.5b04691>)
42. N. Mergu, M. Kim, Y.-A. Son, *Spectrochim. Acta, A* **188** (2018) 571  
(<https://doi.org/10.1016/j.saa.2017.07.047>)
43. T. Keawwangchai, N. Morakot, B. Wannoo, *J. Mol. Model.* **19** (2013) 1435  
(<https://dx.doi.org/10.1007/s00894-012-1698-3>).